Bioorganic & Medicinal Chemistry Letters 24 (2014) 117–121

Contents lists available at ScienceDirect

Bioorganic & Medicinal Chemistry Letters

journal homepage: www.elsevier.com/locate/bmcl

Fluorescent probes of the isoxazole–dihydropyridine scaffold: MDR-1 binding and homology model

Monika I. Szabon-Watola [b], Sarah V. Ulatowski [a], Kathleen M. George [a], Christina D. Hayes [a], Scott A. Steiger [a], Nicholas R. Natale [a,b,*]

[a] NIH COBRE Center for Structural and Functional Neuroscience, The University of Montana, Missoula, MT 59812, United States
[b] Department of Chemistry, University of Idaho, Moscow, ID 83843, United States

ARTICLE INFO

Article history:
Received 18 October 2013
Revised 21 November 2013
Accepted 25 November 2013
Available online 4 December 2013

Dedicated to the memory of Professor Robert O. Hutchins, peerless mentor and good friend

Keywords:
Multidrug resistance transporter
Isoxazole
Dihydropyridine
Homology model

ABSTRACT

Isoxazole-1,4-dihydropyridines (IDHPs) were tethered to fluorescent moieties using double activation via a lanthanide assisted Weinreb amidation. IDHP–fluorophore conjugate **3c** exhibits the highest binding to date for IDHPs at the multidrug-resistance transporter (MDR-1), and IDHP–fluorophore conjugates **3c** and **7** distribute selectively in SH-SY5Y cells. A homology model for IDHP binding at MDR-1 is presented which represents our current working hypothesis.

For three decades 4-aryl-1,4-dihydropyridines (DHPs) have been used as antihypertensive agents which function as antagonists of the L-type voltage gated calcium channel (VGCC).[1] Fluorescent probes of DHPs have been applied to the visualization of the distribution of L-type calcium channels.[2]

The DHP scaffold has also been recognized as a privileged structure and used as for identifying lead hits for several molecular targets.[3,4] In this regard the well established structure activity relationship (SAR) of DHP antagonists of the VGCC[5] can be potentially utilized to design *against* antihypertensive activity, and hence, selectivity for non-calcium channel targets.[6]

The observation that DHPs nicardipine[7] and niguldipine[8] exhibit activity as inhibitors of the multidrug-resistance transporter (MDR-1, also known as p-glycoprotein or P-gp) efflux pump,[9] has stimulated renewed interest in DHPs.[10] Pharmacophore modelling for MDR-1 indicates several common features for inhibitors,[11] notably at least two aryl pockets, and a tether of approximately 3–5 methylenes, leading to another functional group which possesses H-bond donor and lipophilic groups.[12] In contrast, substrates for MDR-1 usually contain a group located near the latter distal end of the tether which is protonated at physiological pH. Of interest to us are the recent observations by the groups of Andrus, and Chmielewski and Hrycyna that bivalent molecules can have significant activity as inhibitors, and that consideration of the tether connection is critical.[13]

Our continuing interest in the bioisosteric 4-isoxazolyl-DHPs[5b,14] (IDHPs) led us to examine a common pharmacophore for DHP MDR-1 inhibitors (Fig. 1), in light of the similarity of the

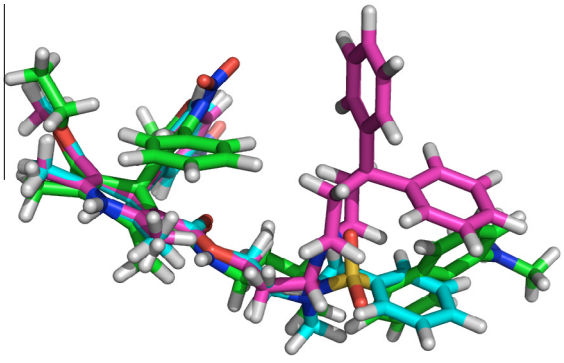

Figure 1. SYBYL common pharmacophore model of nicardipine (cyan) niguldipine (pink), and 3-[4,N-dansyl-1′,4′-butanediamino-]carboxamido-4-Isoxazolyl-DHP **3a** (green).

* Corresponding author.
E-mail address: nicholas.natale@umontana.edu (N.R. Natale).

0960-894X/$ - see front matter © 2013 Elsevier Ltd. All rights reserved.
http://dx.doi.org/10.1016/j.bmcl.2013.11.068

X-ray structure of Isoxazolyl-DHP 1[15] with the general MDR-1 inhibitor model proposed by Ecker,[12] the most striking similarity being the anchor-like conformation of the DHP relative to the C(3) aryl moiety. Recently, we found that IDHPs exemplified by structure **1** are in fact robust ligands of MDR-1,[24] in studies conducted in collaboration with the Psychoactive Drug Screening Program (PDSP), and exhibit an SAR distinct from their activity at the VGCC. In the present study we wished to test the hypothesis as to whether bivalent IDHPs would have enhanced activity at MDR-1.

Double activation preparation of bivalent fluorescent-labeled isoxazolyl-DHPs (IDHPs): The isoxazolyl-DHPs (**1**) can be prepared easily on a multi-gram scale using methods previously reported by our lab,[5b,14–16] however, the direct reaction of the esters is sluggish given their delocalized vinylogous urethane nature. We have found that modest yields can be obtained for **2** using our double activation method,[17] which uses a lanthanide catalyst in the presence of a Weinreb activated amine.[18] The resulting tethered amines can be transformed to fluorophore-labeled analogs quite effectively. Thus, a series of probes with differing tether lengths (**3a–d**), and diverse fluorophores (**3–7**) were readily available. The method, of course, is not limited to isoxazolyl-dihydropyridines, and the *o*-, *m*-, and *p*-bromophenyl DHPs were also converted to dansyl analogs (Supplementary data).[19]

The fluorophores **4–7** were selected to study a range of reactivities in the presence of the IDHP moiety. The 9-anthryl adduct **4** was prepared by reductive amination with sodium cyanoborohydride from amine **2** and anthracene-9-carboxaldehyde.[25] Pyrene-2-carboxylic acid did not give synthetically useful yields with dicyclohexy carbodiimide (DCC), likely owing to steric hindrance, however the corresponding Schotten–Bauman reaction with the

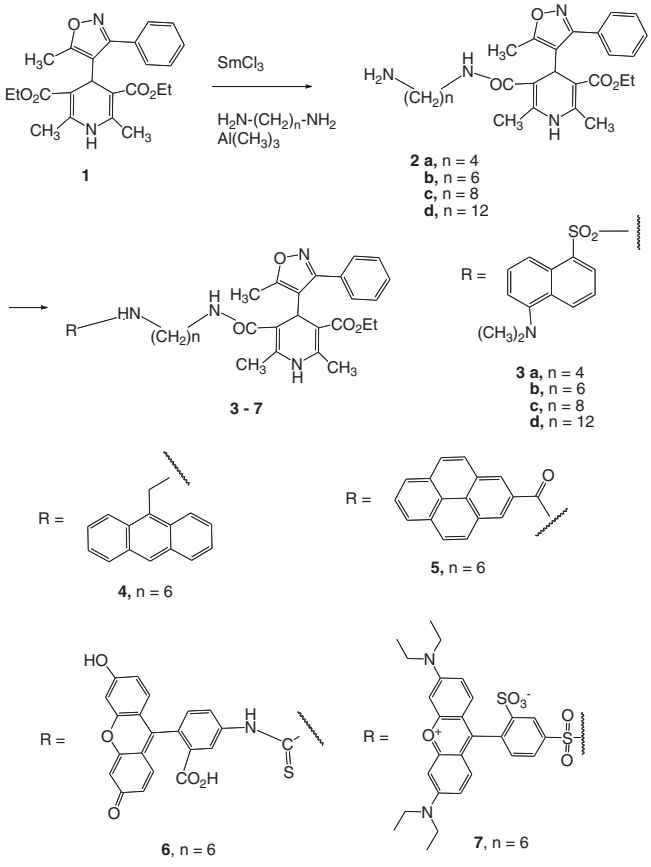

Scheme 1. Synthesis of isoxazole-DHP flourophone conjugates **3–7**.

derived acid chloride proceeded to the amide **5** quite effectively. Fluorescein isothiocyanate (FITC) gave thiourea adduct **6**. Finally sulforhodamine B, similar to the danzyls, proceeded virtually quantitatively to the adduct **7** (Scheme 1).

From a microscopist's perspective, an important consideration in synthesis of a library of fluorophore-conjugated compounds is the extinction coefficient of the fluorophore groups. The extinction coefficient defines how strongly a substance absorbs light at a particular wavelength. Hence, a fluorophore with a high extinction coefficient will enable a microscopist to image a fluorescently labeled compound at a lower, more physiologically relevant concentration than a compound labeled with a fluorophore with a low extinction coefficient. Extinction coefficients of the fluorophores listed in Table 1, span a range from 4400 for dansyl through 85,000 for fluorescein and approximately 120,000 for the sulforhodamines.

Conformational dynamics of the fluorescent probes: The conformational dynamics of IDHPs dramatically effect the topology presented to a biomolecular target.[5b,14–16,24] The danzyl probes, most notably **3c**, in addition to the expected set of signals for the isoxazolyl-DHP, also exhibited a second set of signals with pronounced magnetic anisotropy in typical organic solvents (i.e., $CDCl_3$), and of equal intensity. Nuclear Overhauser spectroscopy evidenced interactions between the DHP C(2) and C(6) methyls with the Isoxazolyl C(3) phenyl, and the isoxazolyl C(3) phenyl with the dimethyl amino groups of the dansyl moiety, indicative of a folded conformation. Raising the temperature resulted in a conformational reorganization to a single set of chemical shifts which were consistent with an extended conformation.[19] The interconversion was not reversible in wet DMSO. Computation indicated that the folded conformation was lower in energy, in the gas phase, consistent with its predominant presence in less polar solvent. The VT and computation are shown in the Supplementar data.

Multidrug-resistance inhibition (MDR-1): MDR-1 inhibition was evaluated in the Psychoactive Drug Screening Program (PDSP) assay, the details of which are given in the Supplementarty data, and described on the PDSP web site http://pdsp.med.unc.edu/pdspw/MDR.php. Compound **3c** exhibited 63% inhibition, versus 0% for untreated cells and 100% for the MDR inhibitor cyclosporin.[21,22] This represents a significant increase in MDR-1 binding compared to IDHP-**1**, which exhibited a value of 48.9% in the PDSP assay.[23,24]

Homology modeling: In the absence of a homo sapien X-ray crystal structure of MDR-1 a homology mode was constructed using *Mus musculus* MDR-1, PDB:3G5U,[26] as a template for threading of the human gene sequence (P08183).[27–29] The sequence alignment was generated using Clustal W,[30] the alignment of and the subsequent threading indicated high sequence homology to the human sequence with a sequence identify of 82.34%. To visualize the hypothetical interactions between **3c** and MDR-1 molecular modeling was conducted. Ligand structures were drawn and energy minimized (Powell method, 0.01 kcal mol^{-1} $Å^{-1}$ gradient termination, MMFF94s force field, MMFF94 charges, 1000 maximum iterations) using the SYBYL software package (Tripos, St. Louis, MO). Virtual dockings of energy-minimized ligand to the MDR-1 homology model were performed using the GOLD software package (Cambridge Crystallographic Data Center, Cambridge, UK)[31] and scored using Chem PLP with default settings. Docking algorithms were performed with the constraint of limiting the allowed binding area to a 6 Å radius around the ARG905 residue. Ligand–receptor ensemble structures were obtained by merging the highest-ranked output ligand orientation structures with the input MDR-1 homology model structure using PyMOL. An MDR-1 human homology model protein active site analysis was performed using Q-site finder.[33] This program binds hydrophobic probes to the

Table 1
Bivalent fluorescent IDHPs prepared for the current study **3–7**

Compds	Fluorophore	Tether length	Empirical formula	Mass spectra (m/Z)[a,b]
3a	Dansyl	4	$C_{37}H_{43}O_6N_5S$	685[M]$^+$
3b	Dansyl	6	$C_{39}H_{47}O_6N_5S$	713[M]$^+$
3c	Dansyl	8	$C_{41}H_{51}O_6N_5S$	741[M]$^+$
3d	Dansyl	12	$C_{45}H_{59}O_6N_5S$	797[M]$^+$
4	9-Anthryl	6	$C_{42}H_{46}N_4O_4$	669[M-1]$^+$
5	2-Pyryl-carboxy	6	$C_{44}H_{44}N_4O_5$	708[M]$^+$
6	Fluorescein	6	$C_{48}H_{47}N_5O_9S$	869[M+1]$^+$
7	SulforhodamineB	6	$C_{54}H_{64}N_6O_{10}S$	1021[M]$^+$

[a] **3a** to **3d** were obtained by FAB MS on a JEOL-JMS-AX505HA.
[b] Compounds **4–7** were obtained by HR-ESMS, Micromass MS/Waters HPLC.

MDR-1 homology model and ranks sites with the most favorable binding energy. These clusters are then placed in rank order of the likelihood of being a binding site according to the sum total binding energies for each cluster. The first binding cluster was bound in the rhodamine binding site or R-site, the second and third sites were located proximal to the nucleotide binding domains (NBDs). The overlap of the dexniguldipine binding site in MDR-1 via photoaffinity labeling (shown in red in Fig. 2),[32] combined with the output of the Q-site finder gave a consensus binding site for IDHP.[33]

Interestingly, the predicted binding location of the IDHP resides near the conserved V907 of Coupling Helix 2, and an essential Mg^{2+} binding residue Q475 of the Walker domain required for ATP hydrolysis. A ligand binding in this location would be expected to limit conformational reorganization necessary for xenobiotic efflux. This presents a testable working hypothesis for future studies, and target design (see Fig. 3).

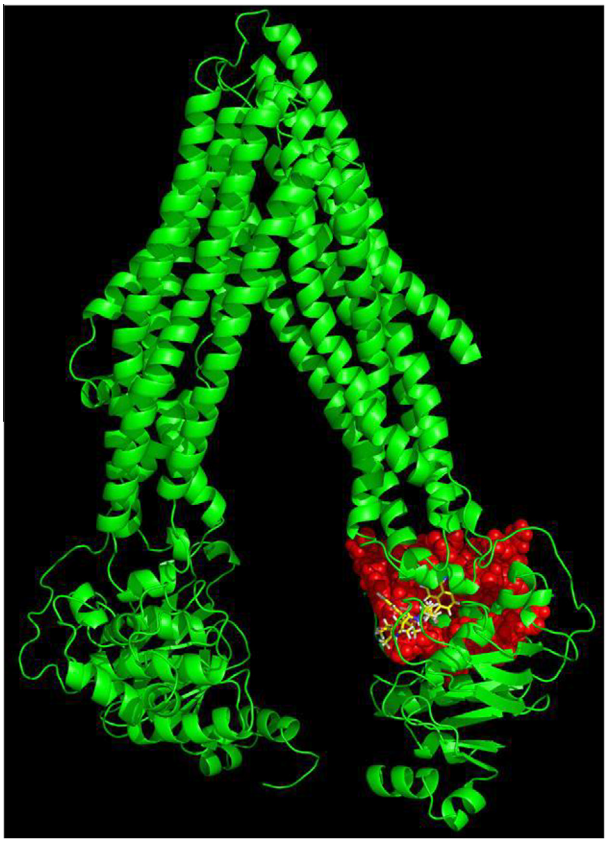

Figure 2. Homology model of IDHP **3c** (gold) docked into MDR-1 based on pdb accession number 3G5U. The red area is the dexniguldipine photoaffinity site.

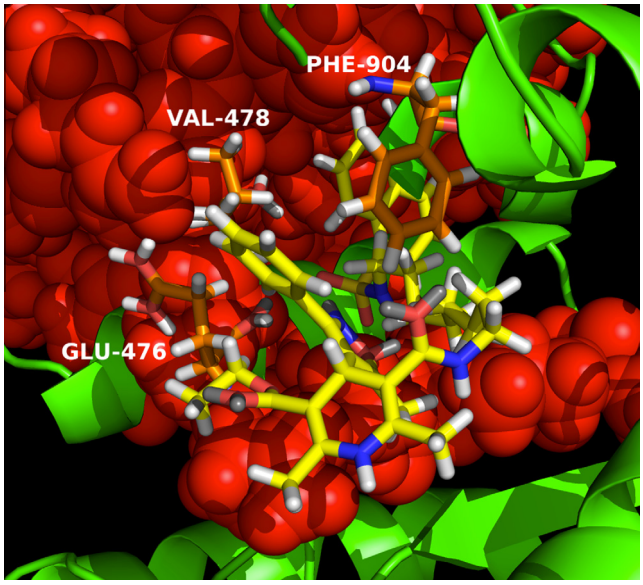

Figure 3. Close up of IDHP **3c** docked into MDR-1. The fluorophore interacts at the edge of the red dexniguldipine photoaffinity site, the DHP moiety of **3c** (gold) is mainly located near the NBD, as predicted by Q-site.

Fluorescent microscopy: SH-SY5Y human neuroblastoma cells (American Type Cell Culture Cat no. CRL-2266) lines were cultured in the recommended media including 10% fetal bovine serum and antibiotics. Cells were plated on coverslips in 12-well plates at 1×10^5/well and allowed to adhere for 48 h. Cells were incubated with DHP–sulfonorhodamine diluted in dimethyl sulfoxide (DMSO) for a prescribed period of time (30 min to 21 h) at 37 °C/5% CO_2. After incubation, media was removed, cells were washed twice with phosphate-buffered saline (PBS), and fixed in 4%

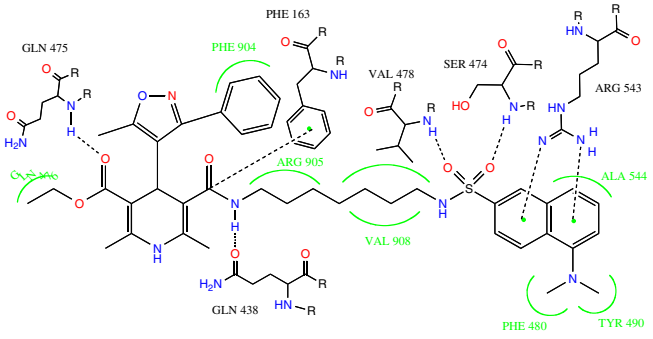

Scheme 2. Summary of close contacts between **3c** and MDR-1 from docking the homology model.

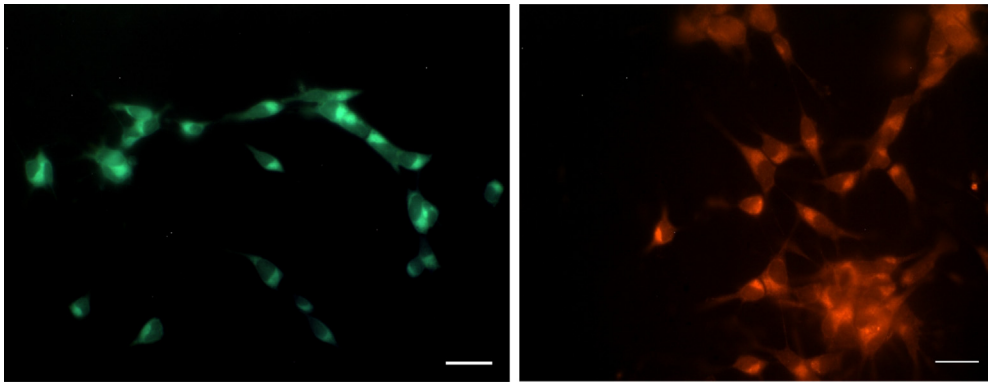

Figure 4. Confocal fluorescence Microscopy of SH-SY5Y cells with: (left), 10 μM dansyl isoxazolyl-DHP **3c** (green); and (right) 1 μM sulforhodamine B-isoxazole DHP 7 (orange), imaged at 60×, with a 90 min incubation time. Scale bar indicates a distance of 10 μm.

paraformaldehyde in PBS (20 min, RT). Fluorescent images were taken with a Nikon Eclipse E800 fluorescent microscope and images were processed with Nuance 1.6.2.368 alpha software (Cambridge Research Institute) (see Scheme 2).

Representative results are shown in Figure 4. Dansyl isoxazole **3c** and Sulforhodamine isoxazole **7** possess fluorophores with radically different physical characteristics, yet they localize in SH-SY5Y cells in virtually identical locations, whereas controls for the fluorophores not conjugated to the IDHP showed non-selective binding throughout the cell. This suggests that it is the IDHP moiety which is the driving force for the localization. The characteristics of the fluorophores were effected by the tether. For example, the sulforhodamine control alone had higher intensity (albeit no selectivity in cellular distribution) compared to the conjugate **7**, with a tether of six methylene units. In contrast the fluorophore conjugate **3c**, with eight methylenes had a higher intensity than the corresponding control (dansylcadaverine), which is consistent with the former being inside of the Forster radius and exhibits quenching relative to fluorophore alone, whereas the latter with the longer tether is beyond this radius.

4-Aryl-DHPs tethered via an ester linkage to the fluorophore BODIPY localized in the L-type calcium channel in a functional, extracellular heparin-binding site.[2] It has previously been reported that expression of MDR-1 is reported to be localized at several subcellular sites, including the nucleus, mitochondria, and Golgi apparatus of rat brain cells and suggests a role in multidrug resistance at subcellular sites.[20] The current study suggests an analogous distribution in SH-SY5Y cells, and will be the subject of future studies.

Summary: Isoxazolyl-DHPs can be readily conjugated to fluorophores, once tethering moieties are connected using a further application of our double activation methodology. A wide variety of fluorophores can be conjugated to the IDHP using this approach. The localization of the conjugates in SH-SY5Y cells appears to be driven by the IDHP moiety. The distribution of the present conjugates are not consistent with previous reports of L-type calcium channels,[2] and appear to concentrated in the nuclear envelope and the Golgi.[20] We have developed a homology model of MDR-1, which combined with our experimental observations, represents our current working hypothesis. Current studies are focused on whether the IDHPs may represent useful tools for the study of MDR-1, and ultimately lead to clinically useful inhibitors. Our progress will be reported in due course.

Acknowledgements

The authors thank NIH for grants NS038444 (N.N., M.I.S.), 5U01ES016102-02 (K.M.G., S.V.U.), and P20RR015583 (N.N., S.S.). C.D.H. thanks the NSF REU Award Number 0649306. M.I.S. thanks the Malcolm and Carol Renfrew Scholarship. We thank Dr. Alex Blumenfeld for VT NMR and Dr. Gary Knerr for able assistance in FAB MS while at the University of Idaho. We thank Dr. Mike Braden and Dave Holley of the Core Facility for Molecular Computation (UM) for helpful discussions during pharmacophore modeling.

MDR1 data was generously provided by the National Institute of Mental Health's Psychoactive Drug Screening Program (NIMH PDSP), Contract # HHSN-271-2008-00025-C (NIMH PDSP). The NIMH PDSP is Directed by Bryan L. Roth MD, Ph.D. at the University of North Carolina at Chapel Hill and Project Officer Jamie Driscoll at NIMH, Bethesda MD, USA.

Supplementary data

Supplementary data associated with this article can be found, in the online version, at http://dx.doi.org/10.1016/j.bmcl.2013.11.068.

References and notes

1. Zamponi, G. *Voltage-Gated Calcium Channels*; Landes Bioscience: New York, 2005.
2. Knaus, H. G.; Moshammer, T.; Friedrich, K.; Kang, H. C.; Haugland, R. P.; Glossman, H. *Proc. Natl. Acad. Sci. U.S.A.* **1992**, *89*, 3586.
3. Kubinyi, H.; Mueller, G. *Chemogenomics in Drug Discovery*; Wiley-VCH: New York, 2004. pp 18–19.
4. Natale, N. R. *Learning from the Hantzsch Synthesis*; Chemical Innovation (American Chemical Society), 2000. pp 22–28.
5. (a) Triggle, D. J.; Langs, D. A.; Janis, R. A. *Med. Res. Rev.* **1989**, *9*, 123; (b) Zamponi, G.; Stotz, S. C.; Staples, R. J.; Rogers, T. A.; Nelson, J. K.; Hulubei, V.; Blumenfeld, A.; Natale, N. R. *J. Med. Chem.* **2003**, *46*, 87.
6. (a) Nagarathnam, D.; Wetzel, J. M.; Miao, S. W.; Marzabadi, M. R.; Chiu, G.; Wong, W. C.; Hong, X.; Fang, J.; Forray, C.; Branchek, T. A.; Heydorn, W. E.; Chang, R. S.; Broten, T.; Schorn, T. W.; Gluchowski, C. *J. Med. Chem.* **1998**, *41*, 5320; (b) Miri, R.; Mehdipour, A. *Bioorg. Med. Chem.* **2008**, *16*, 8329.
7. Nobili, S.; Landini, I.; Giglioni, B.; Mini, E. *Curr. Drug Targets* **2006**, *7*, 861.
8. (a) Zhou, X. F.; Shao, O.; Coburn, R. A.; Morris, M. E. *Pharm. Res.* **2005**, *22*, 1989; (b) Zhou, X. F.; Zhang, L.; Tseng, E.; Scott-Ramsay, E.; Schentag, J. J.; Coburn, R. A.; Morris, M. E. *Drug Metab. Dispos.* **2005**, *33*, 321.
9. Linton, K. J. *Physiology* **2007**, *22*, 122.
10. (a) Shah, A.; Bariwal, J.; Molnár, J.; Kawase, M.; Motohashi, N. *Top. Heterocycl. Chem.* **2008**, *15*, 201; (b) Mehdipour, A. R.; Javindnia, K.; Hemmateenejad, B.; Amirghorfran, Z.; Miri, R. *Chem. Biol. Drug Des.* **2007**, *70*, 337; (c) Voigt, B.; Coburger, C.; Monar, J.; Hilgeroth, A. *Bioorg. Med. Chem.* **2007**, *15*, 5110.
11. (a) Ekins, S.; Ecker, G. F.; Chiba, P.; Swaan, P. W. *Xenobiotica* **2007**, *37*, 1152; (b) Crivori, P.; Reinach, B.; Pezzetta, D.; Poggesi, I. *Mol. Pharm.* **2006**, *3*, 33.
12. (a) Ecker, G.; Huber, M.; Schmid, D.; Chiba, P. *Mol. Pharmacol.* **1999**, *56*, 791; (b) Ecker, G. F.; Schwaha, R.; Demel, M.; Chiba, P. Pharmacoinformatic approaches to target P-glycoprotein: from inhibitor design to substrate prediction. ACS 235th National Meeting, New Orleans, LA, April 6–10, 2008, Abstract MEDI 161.
13. (a) Sauna, Z. E.; Andrus, M. B.; Turner, T. M.; Ambudkar, S. V. *Biochemistry* **2004**, *43*, 2262; (b) Namanja, H. A.; Emmert, D.; Davis, D. A.; Campos, C.; Miller, D. A.; Hrycyna, C. A.; Chmielewski, J. *J. Am. Chem. Soc.* **2011**, *134*, 2976; (c) Pires, M. M.; Emmert, D.; Hrycyna, C. A.; Chmielewski, J. *Mol. Pharmacol.* **2009**, *75*, 92; (d) Pires, M. M.; Hrycyna, C. A.; Chmielewski, J. *Biochemistry* **2006**, *45*, 11695.

14. (a) Natale, N. R.; Rogers, M. E.; Staples, R.; Triggle, D. J.; Rutledge, A. *J. Med. Chem.* **1999**, *42*, 3087; (b) Mirzaei, Y. R.; Simpson, B. M.; Triggle, D. J.; Natale, N. R. *J. Org. Chem.* **1992**, *57*, 6271; (c) Natale, N. R.; Triggle, D. J.; Palmer, R. B.; Lefler, B. J.; Edwards, W. D. *J. Med. Chem.* **1990**, *33*, 2255; (d) McKenna, J. I.; Schlicksupp, L.; Natale, N. R.; Maryanoff, B. E.; Flaim, S. F.; Willett, R. D. *J. Med. Chem.* **1988**, *31*, 473.
15. Schauer, C. K.; Anderson, O. P.; Quincy, D. A.; Natale, N. R. *Acta Crystallogr., Sect. C, Cryst. Struct. Commun.* **1986**, *C42*, 884.
16. Natale, N. R.; Quincy, D. A. *Synth. Commun.* **1983**, *13*, 817.
17. (a) Zhou, P.; Mosher, M. D.; Taylor, W. D.; Crawford, G. A.; Natale, N. R. *Bioorg. Med. Chem. Lett.* **1997**, *7*, 2455; (b) Han, X.; Twamley, B.; Natale, N. R. *J. Heterocycl. Chem.* **2003**, *40*, 539; (c) Han, X.; Li, C.; Mosher, M. D.; Rider, K. C.; Zhou, P.; Crawford, R. L.; Fusco, W.; Paszczynski, A.; Natale, N. R. *Bioorg. Med. Chem.* **2009**, *17*, 1671.
18. (a) Basha, A.; Lipton, M.; Weinreb, S. M. *Tetrahedron Lett.* **1977**, 4171; (b) Lipton, M. F.; Basha, A.; Weinreb, S. M. *Org. Synth.* **1979**, *59*, 49.
19. Szabon-Watola, M. I. Neurotransporters, receptors and calcium signaling. M.S. Thesis, University of Idaho, 2006.
20. Babakhanian, K.; Bendayan, M.; Bendayan, R. *Biochem. Biophys. Res. Commun.* **2007**, *361*, 301.
21. Tiberghien, F.; Loor, F. *Anticancer Drugs* **1996**, *7*, 568.
22. Mizuno, N.; Niwa, T.; Yotsumoto, Y.; Sugiyama, Y. *Pharmacol. Rev.* **2003**, *55*, 425.
23. Hamilton, G.; Cosentini, E. P.; Teleky, B.; Koperna, T.; Zacheri, J.; Riegler, M.; Feil, W.; Schiessel, R.; Wenzi, E. *Anticancer Res.* **1993**, *13*, 2059.
24. Hulubei, V.; Meikrantz, S. B.; Quincy, D. A.; Houle, T.; McKenna, J. I.; Rogers, M. E.; Steiger, S.; Natale, N. R. *Bioorg. Med. Chem.* **2012**, *20*, 6613.
25. Hutchins, R. O.; Natale, N. R. *Org. Prep. Proced. Int.* **1979**, *11*, 201.
26. Aller, S. G.; Yu, J.; Ward, A.; Weng, Y.; Chittaboina, S.; Zhuo, R.; Harrell, P. M.; Trinh, Y. T.; Zhang, Q.; Urbatsch, I. L.; Chang, G. *Science* **2009**, *323*, 1718.
27. (a) Globisch, C.; Pajeva, I. K.; Wiese, M. *ChemMedChem* **2008**, *3*, 280; (b) Sirisha, K.; Shekhar, M. C.; Umasankar, K.; Mahendar, P.; Sadanandam, A.; Achaiah, G.; Reddy, V. M. *Bioorg. Med. Chem.* **2011**, *19*, 3249.
28. Pearson, W. R.; Lipman, D. J. *Proc. Natl. Acad. Sci. U.S.A.* **1988**, *85*, 2444.
29. Sali, A.; Blundell, T. L. *J. Mol. Biol.* **1993**, *234*, 779.
30. Larkin, M. A.; Blackshields, G.; Brown, N. P.; Chenna, R.; McGettigan, P. A.; McWilliam, H.; Valentin, F.; Wallace, I. M.; Wilm, A.; Lopez, R.; Thompson, J. D.; Gibson, T. J.; Higgins, D. G. *Bioinformatics* **2007**, *23*, 2947.
31. Verdonk, M. L. et al *Proteins* **2003**, *52*, 609.
32. Borchers, C.; Boer, R.; Klemm, K.; Volker, F.; Denzinger, T.; Ulrich, W.; Haas, S.; Ise, W.; Gekeler, V.; Przybylski, M. *Mol. Pharm.* **2002**, *61*, 1366.
33. http://www.modelling.leeds.ac.uk/qsitefinder/help.html, last accessed November 7, 2013.
Notes: Experimental for the synthesis of 5-[12-(5-dimethylamino-naphthalen-1-ylsulfamoyl)-dodecylcarbamoyl]-2,6-dimethyl-4-(5-methyl-3-phenyl-isoxazol-4-yl)-1,4-dihydro-pyridine-3-carboxylic acid ethyl ester, **3d**.
Yield from two steps 4%, greenish oil, ratio of two conformers: 80% of folded versus 20% of extended, ^{1}H NMR for **folded** conformation: δ 1.12 (t, J = 6.8 Hz, 3H, ethyl CH_3), 1.18–1.4 (m, 20H, amine 10*CH_2's), 1.35 (m, 4H, amine 2*CH_2), 1.85 (s, 3H, C-2 Me), 2.07 (s, 3H, C-6 Me), 2.41 (s, 3H, isoxazole C-5′ Me), 2.83 (m, 2H, amine CH_2), 2.86 (s, 6H, N $(CH_3)_2$), 2.98 (m, 1H, amine CH), 3.16 (m, 1H, amine CH), 4.00 (m, 2H, $CH_3CH_2CO_2$), 4.55 (m, 1H, NH), 4.81 (br s, 1H, pyridine NH), 4.94 (s, 1H, C-4 CH), 5.19 (br s, 1H, NH), 7.18 (d, J = 7.5 Hz, 1H, naphthalene-H), 7.38 (m, 3H, Ph-H's), 7.51 (m, 2H, Ph-H's), 7.53 (m, 2H, naphthalene-H's), 8.23 (m, 1H, naphthalene-H), 8.30 (m, 1H, naphthalene-H), 8.51 (d, 1H, naphthalene-H). ^{13}C NMR δ 11.34, 14.40, 17.87, 19.76, 26.37, 26.63, 28.88, 29.14, 29.24, 29.29, 29.34 (2C′s), 29.53, 30.73, 39.51 (2C's), 43.34, 45.43 (2C's), 59.63, 98.80, 106.54, 115.20, 118.94, 118.95, 123.23, 127.98 (2C's), 128.31, 128.75, 129.26 (2C′s), 129.64, 129.68, 129.92, 130.34, 130.57, 134.58, 134.59, 145.00, 152.01, 163.11, 166.23, 167.46.
Characteristic peaks for **extended** conformation, ^{1}H NMR: δ 1.00 (t, J = 6.8 Hz, 3H, ethyl CH_3), 2.26 (s, 3H, isoxazole C-5′ Me), 2.52 (s, 3H, C-2 Me), 2.65 (s, 3H, C-6 Me), 4.15 (m, 2H, $CH_3CH_2CO_2$), 7.18 (m, 1H, naphthalene-H), 7.35 (m, 1H, Ph-H), 7.40 (m, 2H, Ph-H's), 7.51 (m, 2H, Ph-H's), 7.55 (m, 2H, naphthalene-H's), 8.21 (m, 1H, naphthalene-H), 8.30 (d, 1H, naphthalene-H), 8.55 (m, 1H, naphthalene-H). ^{13}C NMR δ 11.40, 13.67, 39.61, 127.30(2C's), 129.07, 129.88, 167.02, 168.02. FAB$^+$ (*m*-NBA) *m*/*z* 797.24 [M$^+$], 798.24 [M+1]$^+$, also observed 796.24 [M-1]$^+$. Anal. Calcd for $C_{45}H_{59}O_6N_5S{\cdot}H_2O$: C, 66.23; H, 7.53; N, 8.58. Found: C, 66.02; H ,7.16; N, 8.19.